the general science journal

Conversion of vacuum energy into mechanical energy

By Claus W. Turtur June – 03 – 2008

PACS- Numbers: 41.20.Cv, 84.60.-h, 89.30.-g, 95.36.+x, 98.62.En

Author's address: Prof. Dr. Claus W. Turtur
University of Applied Sciences Braunschweig-Wolfenbuettel
Salzdahlumer Strasse 46 / 48
Germany - 38302 Wolfenbuettel
Email: c-w.turtur@fh-wolfenbuettel.de

Abstract

As generally known, the speed of light is an upper limit for speed at all, also for the propagation of electrostatic and magnetic fields. Retarded potentials are to be understood on this basis. This means, that every electric charge permanently emits electrostatic field and field energy propagating into space with the speed of light. But from where does this energy originate ? In order to answer this question, we follow a package of emitted electrostatic field and we find that it loses energy during propagation. In other words: Space extracts energy from the field. This suggests the explanation, that there is a permanent circuit-flow of energy, within which the field source is supported with energy from space, converts this energy into electrostatic field, and space itself takes back this energy from the field during its propagation. Some part of this energy will remain in space as Coulomb field, but another part will undergo the described flow.
This perception sounds reasonable but unusual. Thus it is proven with a theoretical model, on the basis of which machine is developed, confirming the theory by the fact that it really working. This machine converts energy from this flow in the vacuum into mechanical energy. The rotor described here converts a mechanical power of $1.75 \cdot 10^{-7}$ Watt from vacuum energy into mechanical energy.

Article body

1. Theory

Electrical charge, produces electrical field. The field strength is given by Coulomb's law, if necessary by additional integration over the charge density [1]. This is possible for electrically charged elementary particles as well as for macroscopic charged objects. In the moment, when a charged object begins to exist, the field begins to propagate into the whole space $\mathbb{R}^3$. In this way, the charge emits the field during time. This is also known in connection with the retarded Lienard-Wiechert potential [2]. If a charge is moving, the electrostatic field follows with retardation, namely with the speed of light, otherwise electrostatic fields could be used to transmit information faster than with the speed of light [3]. A further confirmation of the perception that electrostatic fields propagate with finite speed is the fact, that the Hertzian dipole emitter with its characteristics can be explained on the basis of the retarded propagation of the electric and the magnetic fields produced by oscillating electric charges [4,5]. This means, that electrostatic and magnetic fields have the same speed of propagation as electromagnetic waves.

From the field strength, the energy density can be calculated [6], and from there the amount of energy which is emitted per time. Let us do this as following: We consider an electrical charge Q as field source with spherical symmetry, which can be an elementary particle as well as a macroscopic charged sphere (please see Fig.1).
The field strength produced is given by Coulomb's law $\vec{E}(\vec{r}) = \frac{1}{4\pi\varepsilon_0} \cdot \frac{Q}{r^3} \cdot \vec{r}$, where the centre of the charge is located in the origin of coordinates and $\vec{r}$ is the position vector of an arbitrary point in the space at which the field strength shall be determined.

In spherical coordinates with $\vec{r} = (r, \vartheta, \varphi)$, the absolute value of the field strength is dependant not of the direction of $\vec{r}$ but only of its absolute value $r = |\vec{r}|$, namely $E = |\vec{E}| = \frac{1}{4\pi\varepsilon_0} \cdot \frac{Q}{r^2}$.

The energy density of the electric field with spherical symmetry is $u = \frac{\varepsilon_0}{2} \cdot |\vec{E}|^2$.

Consequently the energy density of the field with spherical symmetry is $u = \frac{\varepsilon_0}{2} \cdot |\vec{E}|^2 = \frac{\varepsilon_0}{2} \cdot \left(\frac{1}{4\pi\varepsilon_0} \cdot \frac{Q}{r^2}\right)^2 = \frac{Q^2}{32\pi^2\varepsilon_0 r^4}$.

Now we follow the propagation of a given volume filled with electrostatic field. Let us start our considerations at the time $t = 0$, at which the field has just filled a sphere with radius x_1. Let us compare this with a moment $\Delta t > 0$, at which the field reaches a shell with the radius $x_1 + c \cdot \Delta t$ (c = speed of light), so that during the time interval Δt the emitted energy has the same amount as the energy within the shell from x_1 to $x_1 + c \cdot \Delta t$, because the total energy of the total field was enhanced

by this amount. This amount of energy, which is different from zero, can only be generated by the field source in the center of the sphere, because there is no other source of field and energy.
Remark: This approach for the calculation was chosen, in order to make x_1 independent from the radius of the field source itself. If for instance the field source is an electron, its radius can not be clearly determined, because the classical radius of the electron [7] is in contradiction with values from scattering experiments [8]. We can avoid unnecessary discussions about this problem here by using an x_1 larger than the radius of the field source.

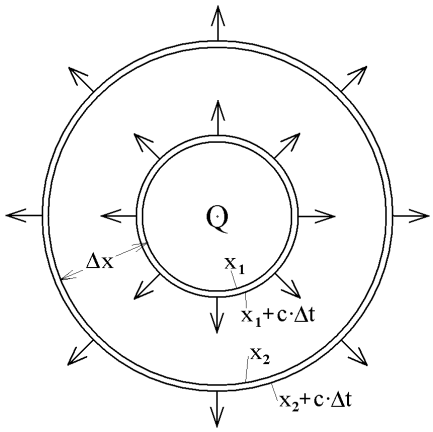

FIG. 1.
Illustration of a spherical shell which contains a certain amount of field energy originating from the charge Q in the centre of the sphere. The sense of this sketch is to trace the field's energy when passing empty space.

The energy within the spherical shell from x_1 to $x_1 + c \cdot \Delta t$, which was emitted during the time interval Δt can now be calculated as the volume integral in spherical coordinates

$$E_{\substack{\text{inner}\\\text{shell}}} = \int_{\substack{\text{spherical}\\\text{shell}}} u(\vec{r})\,dV = \int_{\varphi=0}^{2\pi}\int_{\vartheta=0}^{\pi}\int_{r=x_1}^{x_1+c\cdot\Delta t} \frac{Q^2}{32\pi^2\varepsilon_0 r^4}\cdot r^2\cdot\sin(\vartheta)\,dr\,d\vartheta\,d\varphi$$

$$= \frac{Q^2}{32\pi^2\varepsilon_0}\cdot\int_{\varphi=0}^{2\pi}\int_{\vartheta=0}^{\pi}\underbrace{\int_{r=x_1}^{x_1+c\cdot\Delta t}\frac{1}{r^2}\cdot dr}_{=\frac{c\cdot\Delta t}{(x_1+c\cdot\Delta t)\cdot x_1}}\cdot\sin(\vartheta)\,d\vartheta\,d\varphi = \frac{Q^2}{32\pi^2\varepsilon_0}\cdot\frac{c\cdot\Delta t}{(x_1+c\cdot\Delta t)\cdot x_1}\cdot\underbrace{\int_{\varphi=0}^{2\pi}\underbrace{\int_{\vartheta=0}^{\pi}\sin(\vartheta)\,d\vartheta}_{=2}\,d\varphi}_{=4\pi}$$

$$= \frac{Q^2}{32\pi^2\varepsilon_0}\cdot\frac{c\cdot\Delta t}{(x_1+c\cdot\Delta t)\cdot x_1}\cdot 4\pi = \frac{Q^2}{8\pi\varepsilon_0}\times\frac{c\cdot\Delta t}{(x_1+c\cdot\Delta t)\cdot x_1}$$

Obviously the result is not zero. This means that the source indeed emits energy permanently. It looks somehow paradoxical, because we have to find a source of energy supporting the electrical charge.

We find the possible origin of this energy as following: We trace the energy within the shell from x_1 to $x_1 + c \cdot \Delta t$ by tracking this shell until to the time t' (later than $t_1 + \Delta t$) at which it has expanded to a spherical shell of inner radius x_2 and outer radius $x_2 + c \times \Delta t$. The calculation of the energy within this outer shell now is

$$E_{\substack{\text{outer}\\\text{shell}}} = \int_{\substack{\text{sherical}\\\text{shell}}} u(\vec{r})\,dV = \int_{\varphi=0}^{2\pi}\int_{\vartheta=0}^{\pi}\int_{r=x_2}^{x_2+c\cdot\Delta t} \frac{Q^2}{32\pi^2\varepsilon_0 r^4}\cdot r^2\cdot\sin(\vartheta)\,dr\,d\vartheta\,d\varphi \qquad (\text{with } x_2 = x_1 + \Delta x)$$

$$= \frac{Q^2}{32\pi^2\varepsilon_0}\cdot\int_{\varphi=0}^{2\pi}\int_{\vartheta=0}^{\pi}\underbrace{\int_{r=x_1+\Delta x}^{x_1+\Delta x+c\cdot\Delta t}\frac{1}{r^2}\cdot dr}_{=\frac{c\cdot\Delta t}{(x_1+\Delta x+c\cdot\Delta t)\cdot(x_1+\Delta x)}}\cdot\sin(\vartheta)\,d\vartheta\,d\varphi = \frac{Q^2}{32\pi^2\varepsilon_0}\cdot\frac{c\cdot\Delta t}{(x_1+\Delta x+c\cdot\Delta t)\cdot(x_1+\Delta x)}\cdot\underbrace{\int_{\varphi=0}^{2\pi}\underbrace{\int_{\vartheta=0}^{\pi}\sin(\vartheta)\,d\vartheta}_{=2}\,d\varphi}_{=4\pi}$$

$$= \frac{Q^2}{32\pi^2\varepsilon_0}\cdot\frac{c\cdot\Delta t}{(x_1+\Delta x+c\cdot\Delta t)\cdot(x_1+\Delta x)}\cdot 4\pi = \frac{Q^2}{8\pi\varepsilon_0}\cdot\frac{c\cdot\Delta t}{(x_1+\Delta x+c\cdot\Delta t)\cdot(x_1+\Delta x)}$$

As can be seen by comparison of the denominators, the field energy within the traced shell decreases during propagation into the space. Because the propagating shell is in contact only with space, it means, that space takes the energy from the field. It is clear, that the energy emitted from the field source is constant during time.

In consequence, this suggests the following explanation:
Electrical charge is supported with energy from space and converts this energy (which is at least a part of the energy of vacuum) into electrical field energy. During propagation space takes back some of the energy from the electrical field, but part of the field's energy will still remain as Coulomb-field. The energy of the electrical field is not returned completely back to

the space, because we know that the expanding Coulomb-field still contains some energy, which does not decrease completely to zero, as the field strength will not decrease completely to zero (at every point in the space).

By the way: The propagation of electrical field energy has an analogue in gravitation, at least in Newton's conception. Gravitational fields (with the field strength $\vec{G} = \gamma \cdot \frac{M}{r^3} \cdot \vec{r}$) also have a static field energy with the density $u = \frac{1}{8\pi\gamma} \cdot \left|\vec{G}\right|^2$, and they also propagate into the space with the speed of light (with γ = Newton's constant of gravitation and, with M as gravitational mass). This is known from the work on gravitational waves ([9], [10], [11], [12], [13]). And the gravimagnetic field is known from the Thirring-Lense-effect ([14], [15], [16]).
But let us attend again to the electrostatic field, and look how energy can be extracted from it.

Apostille: The fact, that the mere empty space (the vacuum) contains energy is known from the cosmological constant Λ of the theory of General Relativity [17], and also from experimental investigations of astrophysics [18], [19] (with values being measured in the order of magnitude of about $10^{-9}\,J/m^3$), where the standard model of astrophysics comes to the conclusion, that about 65% of the universe consists of invisible vacuum-energy. And also quantumelectrodynamical considerations regarding the nontrivial structure of the vacuum [20] (see for instance vacuum polarisation) confirm the fact, that the vacuum contains energy. Up to now, there is no clarity about the real value of the energy density, but this open question does not affect the functioning principle of the electrostatic driven motor presented here. In this sense, the electrostatic motor does nothing else, but the conversion of vacuum-energy into mechanical energy. The original purpose of the conception presented here was to find a better understand of the vacuum-energy and maybe to solve the contradictions which are still open between geometrodynamics, quantumelectrodynamics and astrophysics.

1.2. Experimental proposal

If there is really a permanent flow of energy through vacuum by each electrical charge, it should be possible to extract energy from this flow. If somebody would succeed in performing this extraction of energy, this would be proof of the theoretical model introduced above. In order to achieve this proof, a model for an experimental setup is developed in this section. The realization of the experiment and the verification of the proof is presented in the next section.
In [1] and [21] we find a description of the image-charge method, which can be used to calculate electrostatic forces between electrical charge and a metal surface, based on the guidance of the electrical flux by metallic surfaces. The flux-lines are always perpendicular to the metallic surface. According to this method it can be calculated, that a rotor with rotor-blades electrically connected to ground, as shown in Fig.2, experiences a torque if a constant electrical charge q is positioned above the rotor. The geometry of the setup can be optimized for a later experiment, but this rather simple concept is convenient now, because it helps to understand the principle and it is easy to calculate the electric field and the electric potential using Coulomb's law. This avoids errors of misinterpretation of a complicated design.

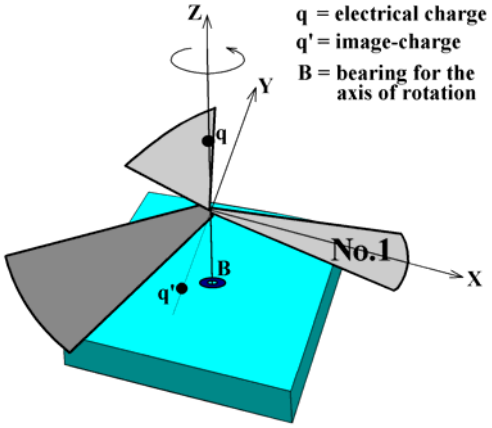

FIG. 2.
Possible setup of an electrostatic motor consisting of a rotor with three metallic blades. An electrical charge q causes a permanent electrostatic force onto the rotor and so it permanently drives the rotor, as long as the practical setup guarantees, that the forces of friction are smaller than the driving electrostatic forces and as long as the charge is kept on its position.
In the picture we see the charge q and the corresponding image-charge q' with regard to rotor-blade No.1.

In order to make the application of the image-charge method as clearly as possible, the rotor blades shall be arranged at an angle of 45° with respect to the xy-plane. Because of symmetry, it is sufficient to perform the calculation with one of the rotor blades. Let us chose rotor blade No.1 being oriented along the x-axis in the moment of consideration. Consequently this blade defines a plane with the functional equation $z(x,y) := -y$. Thus the position vectors of the points of this plane are

$\vec{r} = \begin{pmatrix} x \\ y \\ -y \end{pmatrix}$ with two free parameters $x,y \in \mathbb{R}$.

Because of symmetry of the assembly, considerations for the determination of forces do not alter by principle, when the rotor-blades rotate during time. The axis of rotation is the z-axis, so that all rotor-blades move within the xy-plane.

The charge q is placed at the z-axis with the z-coordinate z_0. The position of the corresponding image-charge q' with respect to the blade No.1 can be found as illustrated in Fig.3. There we see the view from the direction of the x-axis onto the yz-plane. In this view we look at the cut of blade No.1 with the yz-plane being the straight line $z = -y$. Construction of the position of the image-charge q' will lead us to the y-axis, and there to the point with the y-coordinate $y = -z_0$. The x-coordinates of q and q' are zero. Thus the position vector of the charge is $\vec{r}_q = \begin{pmatrix} 0 \\ 0 \\ z_0 \end{pmatrix}$ and the position vector of the image-charge is $\vec{r}_{q'} = \begin{pmatrix} 0 \\ -z_0 \\ 0 \end{pmatrix}$.

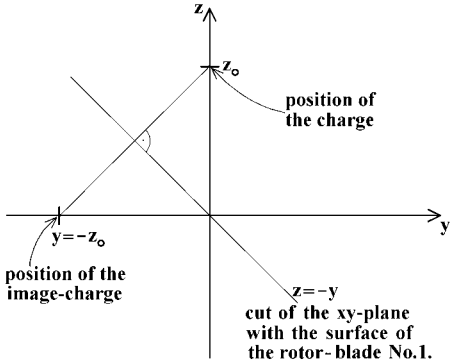

FIG. 3.
Sketch for determination of the position of the image-charge. The charge q as well as the image-charge q' have the x-coordinates $x = 0$.

Using the positions of the field-source q and its image q', we now calculate the forces onto the rotor-blades, by applying Coulomb's law between the charge and the image-charge:

$$\vec{F} = \frac{1}{4\pi\varepsilon_0} \cdot \frac{(+q)\cdot(-q)}{|\vec{r}|^2} \cdot \vec{e}_r \qquad \text{with } \vec{r} = \text{vector from q' to q} \quad \text{and} \quad \vec{e}_r = \text{unit - vector in the direction of } \vec{r},$$

$$\text{where } |\vec{r}| = \sqrt{2}\cdot z_0 \;\Rightarrow\; |\vec{r}|^2 = 2\cdot z_0^2 \qquad \text{and} \quad \vec{e}_r = \begin{pmatrix} 0 \\ \sqrt{1/2} \\ \sqrt{1/2} \end{pmatrix} \text{ with } |\vec{e}_r| = 1.$$

$$\Rightarrow \vec{F} = \frac{1}{4\pi\varepsilon_0} \cdot \frac{-q^2}{2\cdot z_0^2} \cdot \begin{pmatrix} 0 \\ \sqrt{1/2} \\ \sqrt{1/2} \end{pmatrix} = \frac{-q^2}{\sqrt{128}\cdot\pi\varepsilon_0 z_0^2} \cdot \begin{pmatrix} 0 \\ 1 \\ 1 \end{pmatrix} \quad \text{for the force between charge and image-charge.}$$

The crucial point is: The charge q as well as the rotor-blade feels a component of the force in y-direction, which causes a rotation of the rotor-blades around the z-axis. For illustration we look again at Fig.2. The force is attractive, because the image-charge has the opposite algebraic sign than the charge itself. From this consideration we understand the direction of the rotation as indicated with a bent arrow in Fig.2.

Up to now the text was an explanation of the principle, but for a real experimental setup, it is necessary to optimize the arrangement in order to achieve forces strong enough to be measurable at all. Fig. 4 shows a setup which is a compromise between the effort to enlarge the torque and necessity to find a setup easy to realize for a first experiment. The choice of dimensions is done with regard to experimental conditions.

For the calculations to optimize the geometry an algorithm has been developed applying the image-charge method. By these means an optimization of the field geometry and of the rotor has been conducted. The results of this calculation have been verified successfully with ANSYS [22].

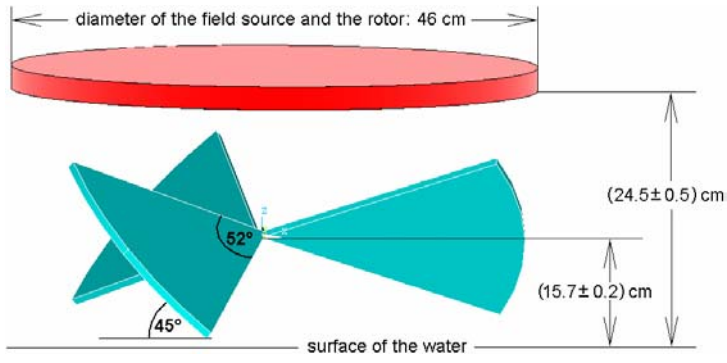

FIG. 4.
Principle design of an electrostatic rotor for the conversion of vacuum-energy into mechanical energy. The disc (red) is electrically charged, whereas the rotor (blue) is connected to ground. The specified dimensions represent the values in the setup of the experiment described.

Although the torque is already optimized to some degree, it is still very small and thus the rotor requires bearing with very low friction, otherwise it would not spin. For a design as given in Fig.4 and a voltage of $U=2kV$ the finite element simulation leads to a torque expectation of about $M=|\vec{M}|=1.8\cdot10^{-6}Nm$, with an uncertainty of perhaps a factor of 2 or 3 because of the numeric approximation.

Further expectations as results from the numerical simulations are the proportionalities
Torque $M\propto U^2$, and thus: power $P\propto U^2$ (with U = electrical voltage)
Torque $M\propto R^2$, and thus: power $P\propto R^2$ (with R = diameter of the rotor)
Thus an enhancement of the voltage to $U=10kV$ would lead to a torque of $M=|\vec{M}|=4.5\cdot10^{-5}Nm$. However high voltage provokes the risk of ionisation of gas molecules as long as the experiment is carried out in air, which would disturb the spinning of the rotor spin because of electrohydrodynamic effects [23]. Consequently, the aim of planning an experiment is, to develop a setup, which is expected to surmount friction but not to ionize gas. A future perspective will be to perform the experiment under vacuum (without gas molecules) in order to allow higher voltage and to exclude the electrohydrodynamic effects for sure.

2. Experimental

2.1 Apparatus description

The result of chapter 1.2 oblige to search a bearing with friction as low as possible with regard to the torque. A first idea could be an air-bearing, because this type is known to produce the lowest friction of all bearings. But it would demand the use of compressed air with the risk to provoke air blasts that might drive the rotor. This is not sensible. We should have in mind, that precautions have to be taken to avoid thermally induced convection of gas moving to rotor. Two possible alternatives appeared, namely a toe-bearing with a glass moving relatively to a metal tip and a hydrostatic bearing. Both types have been realized. The hydrostatic bearing proved to be the easier one in operation, and it was more reliable during operation.

But now, some of the details regarding both of the bearings shall be discussed:
The toe-bearing consists of a contact between glass and metal having a typical coefficient of stiction of about $\mu_S=0.5\ldots0.7$. The rotor has to be built as light as possible in order to minimize friction, for instance with a weight of $m=10^{-2}kg$ (or less). Then the force of static friction would be $F_S=\mu_S\cdot m\cdot g=0.7\cdot10^{-2}kg\cdot10\frac{m}{s^2}=7\cdot10^{-2}N$. If the steel needle has a tip radius of $r=10\mu m$ the torque will be $M_S=7\cdot10^{-2}N\cdot10^{-5}Nm=7\cdot10^{-7}Nm$. This would be just even sufficient to allow rotor with the dimensions of Fig. 4 to spin.

It is not easy to mount such a large rotor on such a small toe-bearing. Furthermore the mechanical adjustment of the rotor relatively to the field source is very critical. So the alternative was conceived to put the rotor on little floating bodies of polystyrene and to set the whole arrangement on the surface of water. This makes the mechanical adjustment of the rotor easy, because the rotor can only move exactly horizontally. Now the field source being a plane disk can be aligned exactly horizontally. Mechanical asymmetries should be as small as possible (at least less than one millimetre in our setup), because they tend to arise asymmetries of the electrostatic field which would attract the rotor until its position within the electrostatic potential finds the minimum of energy. If the torque caused by such an asymmetry is stronger than the torque which drives the rotor minus the torque of friction, the rotor would stop at the position of the minimum of the electrostatic potential. If is self-evident that this has to be avoided in any case.

The system of the swimming rotor has the further advantage that a lateral drift of the rotor turned out to be unproblematic, because the attractive forces of the field-source adjust the rotor below the center of the field source by alone. This self-centering capability is also an aid for proper adjustment.
Fig. 5 is a photograph of the experimental setup of the rotor swimming on polystyrene – with one difference to the experiment from which the results are plotted below. In the picture a metal rod for the purpose of lateral adjustment of the rotor can be seen, which is guided by a glass cylinder positioned vertically under the surface of the water. Because of the self-centering mechanism described above, the glass cylinder turned out to be dispensable. Actually the movement of the rotor was achieved easier without the glass cylinder, because the contact between the glass and the metal rod disturbed the movement of the rotor. Consequently the cylinder was removed for further measurements.
The field source was made from pasteboard covered with aluminium foil. The rotor was made as a frame of balsa wood carrying aluminium foil. The rotor has a weight of $m=8.7Gram$, but three Styrofoam cuboids (each of 0.56 Gram) also perform the rotation. Thus the moment of inertia for rotation is approximately $J\approx3.2\cdot10^{-4}kg\cdot m^2$.

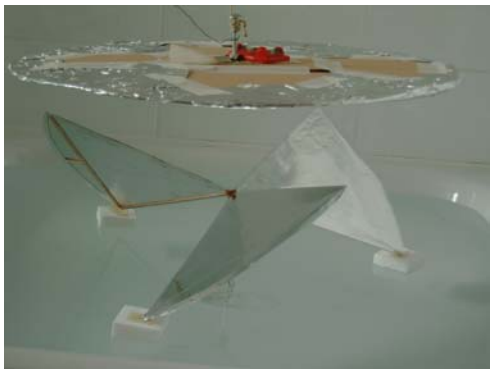

FIG. 5.
Photo of the electrostatic rotor and the field source as used in the experiment. It was a rather simple handmade setup, but it was capable to perform the rotation successfully and reproducible.

2.2 Measurements and results

The field source was charged electrically by connecting it to an electric potential. The rotor swimming on polystyrene was connected to ground together with the water. The rotation observed was controlled with the naked eye, with which it is easy to recognize steps of 60° of rotation by observing the passage of the rotor at a given point. The time of each passage of the rotor has been written by hand and graphically displayed in Fig. 6.
The variance of the data points with regard to a smooth line arises from the fact that the rotor performs lateral oscillations around the optimum position of adjustment due to the self-adjustment mechanism by the attractive force of the field. (By the way: This attractive force is argument to exclude the Biefeld-Brown effect, because ionized gas molecules can not attract the rotor into the centre below the field source.)

Furthermore it should be mentioned, that the electrical voltage between the field source and the rotor was decreasing during time. In the example of Fig. 6, the following happened: At the beginning a voltage of $U=7\text{kV}$ was applied, and the rotor began to move. After approximately half an hour 6…8 revolutions have been fulfilled, and the data acquisition started at a moment at which the voltage was $U=6\,\text{kV}$. During the following hour of data acquisition, the voltage further decreased to $U=4.5\text{kV}$. Consequently the angular velocity of the rotation also decreased during time, (Fig. 6). The decrease of the voltage had technical reasons within the power supply.

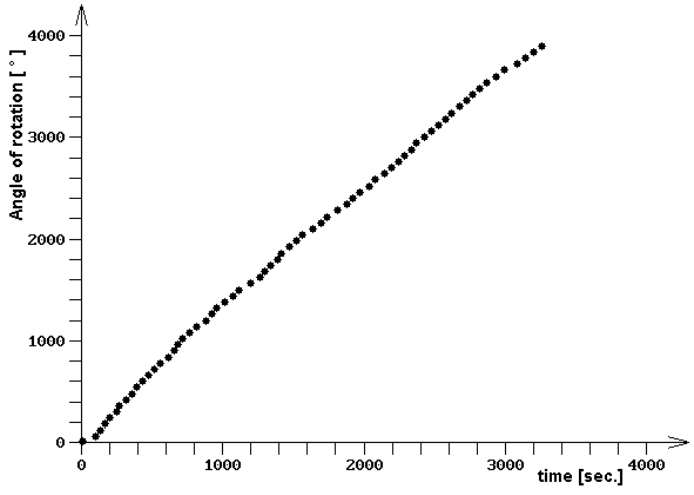

FIG. 6.
Example for the measurement of the rotation under the circumstances explained above. The angle of the rotation is given in degrees, so that one complete revolution corresponds to 360°.

Numerical estimation to comment the results:
From chapter 2.1 we know the valuation of the moment of inertia of about $J \approx 3.2 \cdot 10^{-4} \text{kg} \cdot \text{m}^2$. A torque of $M = 1.2 \cdot 10^{-5} \text{Nm}$, corresponding to a voltage of $U=5\,\text{kV}$ (as a result of the finite element calculations), leads to an angular acceleration of about $\alpha \approx 2.1°/\text{sec.}^2$. The average angular velocity observed in the measurement was about $\omega \approx 0.84°/\text{sec.}$ This means that the rotor reaches its final angular velocity rather fast, due to the hydrostatic friction of the water. Such a short phase of acceleration can not be measured with the naked eye, and this is, what was seen: There was not a slow or long phase of acceleration.
The average engine power converted from the vacuum energy can be estimated from the torque and the angular velocity: $P = M \cdot \omega = 1.75 \cdot 10^{-7} \text{Watt}$, which finally was absorbed by the water via hydrostatic friction.

Additional observation, regarding the criterion of technical energy gain:
If the voltage between the field source and the rotor blades is enhanced to 10 … 20 kV an electrostatic breakthrough can occur, disturbing the continuous movement of the rotor. Thus it is necessary, to investigate whether some electrohydrodynamic effects influence the rotor. A final decision about this question can be extracted from the criterion of technical energy gain as following.

Measurements with a pico-amperemeter have been tried to determine the electric current (which are due to isolation losses). The product of the observed voltage and current was in the order of magnitude of $U \cdot I \approx 10^{4} V \cdot 10^{-6} A \cdot 10^{-2} W$, which is much larger than the power converted from the vacuum. This product of $U \cdot I$ could be modified significantly (for instance by a half or a full order of magnitude) by mounting an isolator between the field-source and the rotor without causing a significant change of angular speed of the rotation. But the final criterion for the technical usability of the rotor is the net energy gain; this means, that the produced energy (per time) has to be more than the energy loss (per time) wheresoever. If this criterion is fulfilled, it is also sure, that there is no classical energy source driving the electrostatic vacuum-rotor, but that really vacuum-energy is driving the rotor.
In order to approach to this goal, the field source was replaced by an electret, which does not enable electric currents in the range of pico-amperes (or more). The electret which was used, was a balloon filled with air (as children use for playing). This material was rubbed on its surface until its electrostatic charge and potential was enough to keep the balloon at the bottom side of ceiling of a room against gravitation. Thereafter the balloon was positioned (by hand) above the rotor as field source, and it made the rotor spin, but only for one or two (not more than two and a half) revolutions. The rotation of the rotor stopped when the rotor came to a minimum of energy. The rotation did not run out continuously, but it stopped because of electrostatic forces, and sometimes the movement could be restarted for another half or one revolution by moving the charged electret-balloon a little bit. This indicates, that the charge on the surface of the balloon was distributed rather inhomogeneously. This inhomogeneity of the charge distribution is confirmed by the fact, that the balloon turns itself to an energetically minimal position when being brought into contact with the ceiling.
The observed movement (of not more than three revolutions) is not enough to claim, that a permanent rotation for the conversion of vacuum-energy was already generated with an electrically charged electret, but it is enough to exclude, that the effect of electrostatic rotation is caused by the Biefeld-Brown-effect or by some electrohydrodynamic reasons, because there is no electric current and thus no conventional electric power driving the rotor, with the field source being an electret.
The possible current caused by an electrically charged air balloon can be estimated to the following upper limit.
Its capacity is known from its shape: $C = 4\pi\varepsilon_0 \cdot r$ (with a balloon radius of $r \approx 10 cm$).
Its voltage might be about $U \approx 10 kV$ (rough but safe estimation, probably it is less).
The duration for which the balloon is sticking to the ceiling is up to half a day: $t \approx 3 \cdot 10^{4} sec.$
Capacity and voltage lead to an electric charge on the surface of $Q = C \cdot U \approx 10^{-7} C$.
This limits the current to $I = Q/t < 3 \cdot 10^{-12} A$.
The arithmetic operator "<" is used because the balloon is not completely discharged when the balloon is falling down. Furthermore the balloon is in mechanical contact with the ceiling as long as the electrical current is running, but the balloon is several centimetres away from the rotor, which means, that the current between the balloon and the rotor is for sure remarkably smaller than the current between the balloon and the ceiling.
The corresponding electric power is $U \cdot I < 3 \cdot 10^{-8} W$. This is not enough to explain the mechanical power of the rotation. This test was made with a rotor supported by a mechanical toe-bearing as shown in Fig.7, which converted even more than the rotor with the hydrodynamic bearing, i. e. it converted more than $1.75 \cdot 10^{-7} W$.

Further investigation (with a small rotor on a toe-bearing):
An other possibility to get better isolation in order to reduce the isolation loss of electrical charge is, to bring the electrostatic rotor into vacuum. Therefore a hydrostatic bearing with water is impossible. Hence a setup with a toe-bearing has been tested, with rotor blades having a surface of 3.5cm x 6.0cm, positioned within a distance of 3.8 … 4.0 cm below the field source. The toe-bearing was taken out of a small commercial Crooke's radiometer, where the tip of a steel needle is in contact with a glass surface. A photo of this setup can be seen in Fig. 7. The rotor begins to spin even with a voltage of 1100 Volt. The voltage was chosen that low in order to avoid the ionization of gas molecules. This rotation needs very good mechanical adjustment, otherwise the rather small rotor blades do not provide enough torque to surmount the friction plus the asymmetries of the electrostatic field.

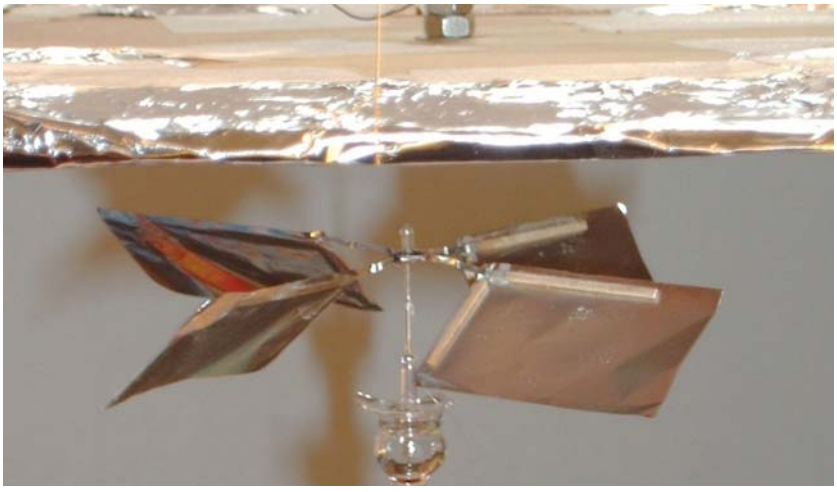

FIG. 7.
Setup of an electrostatic rotor with a toe bearing, supporting four rotor-blades, being positioned below a flat field source. [2]

3. An analogon: A rotor driven by magnetic forces

In [24] and [25] it was demonstrated that the magnetic field and its energy undergoes a similar perpetual cycle of field-energy being transported through the space, as the electrostatic field. A permanent magnet is being permanently supplied with energy from the space, and the space re-absorbs some of the energy from the field during its propagation. Thus it should be expected, that in analogy to the electrostatic rotor the conversion of vacuum-energy into mechanical energy should also be possible with a magnetic rotor, which converts vacuum-energy via the energy of a magnetic field into mechanical energy.

The rotation of the electrostatic rotor had been explained by calculating the forces acting onto the rotor-blades made of electrically conducting material with the use of the image-charge method. This method can be applied because of the fact, that the electric flux coming from outside onto the surface of the material rearranges the electrical charge distribution on the surface in such a way, that the flux-lines are always perpendicular to the conducting surface. The force between the charge and the image-charge explains the rotation of the rotor-blades and thus the conversion of vacuum-energy.

In analogy with these considerations, we regard the Meissner-Ochsenfeld-effect occurring on the surface of a superconductor in a magnetic field [26], which is based on the appearance of superconducting currents on the surface of the superconductor. These currents evoke magnetic fields themselves, which compensate the external magnetic field, so that in the inside of the superconductor the total magnetic field is zero. In this sense, a superconductor displays ideal diamagnetic behavior with $\chi = -1$ (see [27]). The magnetic field caused by the Meissner-Ochsenfeld-effect can be understood as an "image-field" in analogy with the image-charge of image-charge method.

An example was calculated, with a setup as shown in Fig.8. For the sake of simplicity, the external magnetic field driving the rotor shall be premised to be homogeneous (with an arbitrarily chosen numerical value of $|\vec{H}| = 10^3 \frac{A}{m}$), and it shall be orientated along the z-axis. Thus the vector of the magnetic field is the same on all positions everywhere on the surface of the rotor-blades. Consequently the magnetic field produced by the Meissner-Ochsenfeld-effect is orientated into the negative z-direction for all positions of the rotor-blades. For the calculations of the forces the field source and the rotor-blade was subdivided into finite elements. The position-vectors from all individual elements of the field source to all individual elements on the surface of the rotor-blades are going into individually different directions. And each rotor-blade is not symmetric with regard to the z-axis. Consequently the total force acting onto each rotor-blade, which is the sum of all forces acting between each individual elements contains a tangential component which is not orientated into the z-direction. This component will give rise to a rotation of the rotor.

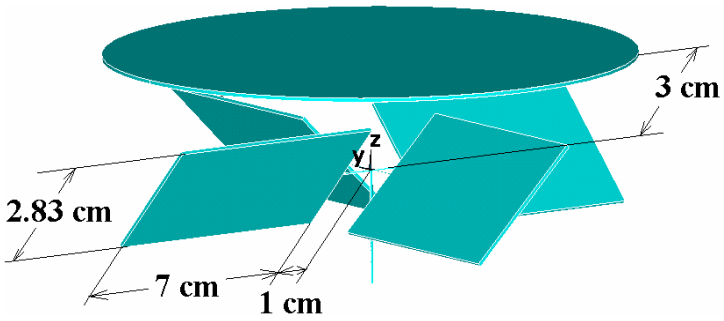

FIG. 8.
Visualization of a superconducting rotor, which is mounted on an axis below a flat permanent magnet. The dimensions will be used for a numerical example.

The forces are repulsive, because the flux-lines cannot penetrate into the ideal diamagnetic material. This is generally known from the Meissner-Ochsenfeld-effect, and it is independent of the polarity of the flat permanent magnet above the rotor. Thus the direction of the rotation is counterclockwise (other than the electrostatic rotor).

The forces are calculated between the two interacting magnetic fields with the usual formula for each pair of finite elements, with H_1 being the field produced by the field source and H_2 being the field produced by the Meissner-Ochsenfeld-effect, so the forces between each pair of elements are

$\vec{F}_{12} = 4\pi\mu_0 \cdot |\vec{r}_{12}|^2 \cdot (\vec{e}_{12} \times \vec{H}_1) \times \vec{H}_2$, with $\mu_0 = 4\pi \cdot 10^{-7} \frac{Vs}{Am}$, $\vec{r}_{12}$ = vector from the field source to the rotor blade

$\vec{e}_{12}$ = unit vector from the field source to the rotor blade.

Thus the total force will be calculated as the sum: $F_{tot} = \sum_i \sum_j \vec{F}_{ij}$.

The homogeneous field in our example ($\vec{H}_1 = -\vec{H}_2 = 10^3 \frac{A}{m} \cdot \vec{e}_z$), allows rather unproblematic summation, leading to the result of $F_R = 4.2 \cdot 10^{-2}$N for the radial component of the force and $F_T = 3.1 \cdot 10^{-4}$N for the tangential component of the force per each single rotor blade. The radial component of the force is compensated by the mechanical axis of the rotor, whereas the tangential component of the force makes the rotor spin. The torque onto the rotor was calculated by summing up the torque

of each pair of finite elements together with its individual radii of rotation. Taking four rotor blades into account, we come to a torque of $M = 5 \cdot 10^{-5} \mathrm{Nm}$. This should be suitable for measurement.

The reason for the restriction of the magnetic field to an absolute value of $10^3 \frac{\mathrm{A}}{\mathrm{m}}$ is the critical magnetic induction B_c regarding the Meissner-Ochsenfeld-effect. For instance Pb has $B_c = 0.080\,\mathrm{T}$ and Al has $B_c = 0.01\,\mathrm{T}$ (for temperature extrapolated $T \to 0\mathrm{K}$), which are examples of superconductors type 1. In order to keep some safety distance from the critical field strength, and in order to respect the fact that the temperature in a real experiment is not zero, a magnetic induction of few milli Tesla might seem possible, corresponding to a field strength in the order of magnitude of $H_1 \approx 10^3 \frac{\mathrm{A}}{\mathrm{m}}$.
If cooling should be made as easy (with liquid nitrogen), it could be interesting use a high-temperature superconductor, as for instance $\mathrm{YBa_2Cu_3O_7}$, which is known as a superconductor type 2. It only behaves as an ideal diamagnet as long as the Shubnikov-phase is avoided. Nevertheless the field strength and with it the maximum reachable forces and the torque can be even a bit larger than with the superconductor type 1 as mentioned above. This also seems sufficient for measurement.

Now the question might arise, whether also a conventional dia-, para-, and ferro- magnetic material might allow to build a rotor, which will rotate in a magnetic field. Dia- and paramagnetic materials have rather low susceptibility (copper: $\chi = -1 \cdot 10^{-5}$, bismuth: $\chi = -1.5 \cdot 10^{-4}$, platinum: $\chi = +1.9 \cdot 10^{-6}$ or aluminium: $\chi = +2.5 \cdot 10^{-4}$, see [28]), but the field strength H_1 could be enhanced perhaps to $10^6 \frac{\mathrm{A}}{\mathrm{m}}$ of even more, because there is no critical field strength. With $|H_2| = |\chi \cdot H_1| \approx 10^{-6} \ldots 10^{-4} \cdot |H_1|$, the product of the field strength of the finite element pair will be about $|H_2 \cdot \chi \cdot H_1| \approx 10^6 \frac{\mathrm{A}}{\mathrm{m}} \cdot \left(10^{-6} \ldots 10^{-4}\right) \cdot 10^6 \frac{\mathrm{A}}{\mathrm{m}} = 10^6 \ldots 10^8 \left(\frac{\mathrm{A}}{\mathrm{m}}\right)^2$. If we keep in mind, that the torque $|M|$ scales with the proportionality $|M| \propto |H_2 \cdot \chi \cdot H_1|$, the torque can be brought to an absolute value comparable with this of a rotor made of superconducting blades or even more. Nevertheless it remains somehow uncertain, whether a rotor of conventional dia- or paramagnetic material can be made sufficient to rotate in permanent magnetic field, because the theoretical considerations for the explanation of the principle of the rotor have been developed for an ideal diamagnet as it is only a superconductor. This is also the reason, why we do not want to think detailed about a rotor made from ferromagnetic material (with ferromagnetic domains) here.
Furthermore, for a practical experiment with a magnetic rotor, it should be kept in mind, that one of the results of the above calculation is, that the tangential component of the force (causing the rotation) is about two orders of magnitude larger than the radial component of the force (disturbing the rotation). Thus it is essential for the construction of the mechanical arrangement. The components have to be prepared and mounted with extremely high precision in order to avoid that the radial forces will prevent the rotation in the following way: Deviations from the ideal exact movement of the rotor have to be kept such small, that the rotor will not find a minimum of energy at some position, which stops its rotation. Forces keeping the rotor in the position of an energy minimum because of tolerances and uncertainties in the mechanical setup have to be smaller than the driving radial forces. This problem of a magnetic rotor being stopped in a minimum of energy regarding the tangential force was already practically experienced (with a setup of low precision).

4. Résumé and discussion

The principle of conversion of vacuum-energy into mechanical energy was theoretically developed and experimentally demonstrated, using an electrostatic principle driving an electrostatically charged rotor.
One the one hand, this has consequences for the understanding of fundamental physics, especially regarding the theory of vacuum, vacuum energy and its connection to electrodynamics and maybe for other fundamental interactions, which also produce fields containing field energy.
One the other hand, it has consequences for technical energy production. If the assembly can be built up with adequate precision, and if electrical isolators can be used, which minimize a loss of electrical charge from the field source, production of mechanical power might be possible in a way that vacuum energy is converted into mechanical energy.
For an optimization regarding the technical application, the setup should be brought into the vacuum, which is known to be a very good isolator. There the voltage could be enhanced by about some orders of magnitude. Because the torque and with it the mechanical power output is proportional to the voltage, this should lead to suitable power production. A further advancement in power production can be expected from enlarging the rotor, because the power is expected to be proportional to the diameter of the rotor, and further benefit might be expected from optimizing the shape of the assembly, especially of the rotor.
An alternative possibility for power production might be the use of a magnetic rotor, because such a device could be driven with a permanent magnet.

References

1. J. D. Jackson, *Klassische Elektrodynamik,* (Walter de Gruyter Verlag, 1981)
2. L. D. Landau and E. M. Lifschitz, *Lehrbuch der theoretischen Physik,* (Verlag Harry Deutsch, 1997), vol.2, Klassische Feldtheorie
3. W. Engelhardt, arXiv:physics.gen-ph/0511172v1, (2005)
4. P. Leuchtmann *Einführung in die elektromagnetische Feldtheorie,* (Pearson Studium, 2007)
5. K. Kark *Grundbegriffe der Antennentechnik, Antennen und Strahlungsfelder,* (Springer Verlag, 2007)
6. R. P. Feynman, R. B. Leighton und M.Sands, *Feynman Vorlesungen über Physik* (Oldenbourg Verlag, 2001), vol.2: Elektromagnetismus und Struktur der Materie
7. P. J. Mohr and N. J. Taylor, Rev. Mod. Phys.72 (2) 351 (2000).
8. E. Lohrmann *Hochenergiephysik,* (B. G. Teubner Verlag, 2005)
9. A. Abramovici et. al., Science 256,325 (1992)
10. F. Acernese et. el., Classical and Quantum Gravity 19, 1421 (2002)
11. M.Ando and TAMA collaboration, Classical and Quantum Gravity 19, 1409 (2002)
12 R.Barish and R.Weiss, Phys. Today 52, 44 (1999)
13. B.Willke et. al., Classical and Quantum Gravity. 19, 1377 (2002)
14. F. Everitt, Gravity-Probe-B Experiment, http://einstein.stanford.edu/index.html
15. U. E. Schröder *Gravitation,* (Wissenschaftlicher Verlag Harri Deutsch, 2002)
16. H. Thirring and J. Lense, Phys. Zeitschr. 19, 33-39 (1918)
17. H. Goenner *Einführung in die Spezielle und Allgemeine Relativitätstheorie,* (Spektrum Akademischer Verlag, 1996)
18. D. Giulini and N. Straumann, arXiv:astro-ph/0009368 (2000)
19. M. Tegmark, arXiv:astro-ph/0207199 v1 (2002)
20. A.Di Giacomo, H.G.Dosch, V.I.Shevchenko, Yu.A.Simonov http://arxiv.org/abs/hep-ph/0007223
21. R.Becker and F. Sauter *Theorie der Elektrizität,* (Teubner-Verlag, 1973)
22. J. Swanson, *Finite Element Program ANSYS* (ANSYS, Inc. Software Products 1970-2008) http://www.ansys.com
23. T. T. Brown *Electrostatic Motor,* U.S.Patent 1,974,483 (Sept. 25.1934)
24. C. W. Turtur, arXiv:physics/0710.3253 v1 (Okt.2007)
25. C. W. Turtur, PHILICA.COM, 113, (Dec. 2007)
26. P. A. Tipler and R. A. Llewellyn, *Moderne Physik* (Oldenbourg Verlag, 2003)
27. R. Kassing et. al., *Bergmann-Schäfer Lehrbuch der Experimentalphysik, Band 6* (Walter de Gruyter Verlag, 2005)
28. H. Stöcker, *Taschenbuch der Physik,* Verlag Harri Deutsch (2007)